DOI 10.4430/bgo00362

Trend surface fitting of airborne gamma-ray spectrum based on 2D-AsLS

K. Sun[1], L.Q. Ge[1], Q.X. Zhang[1], Q.H. Yang[2], Y. Gu[1] and W.C. Lai[1]

[1] *The College of Nuclear Technology and Automation Engineering, University of Technology, Chengdu, China*

[2] *Nuclear Industry Geological Bureau of Jiangxi Province, Nanchang, China*

(Received: 5 January 2021; accepted: 31 May 2021; published online: 28 October 2021)

ABSTRACT The trend surface analysis is one of the important methods for processing radioactive element concentration data of airborne gamma-ray spectrum. At present, the fitting of trend surface is mainly based on the polynomial least-squares method. Due to the degree of limitation of polynomial functions, the polynomial least-squares method is imprecise in describing the trend surface. Therefore, as an alternative approach, we considered the 2D asymmetric least squares (2D-AsLS) developed under 2D tensor product of a P-spline. 2D-AsLS can make full use of the spatial characteristics of radioactive element concentration data to fit trend surfaces. 2D-AsLS can adjust the fitting effect of the trend surface by modifying smoothness, and can evaluate the fitting effect through the parameters (i.e. fitting coefficient, error variance, coefficient of variation, and degree of deviation). Gamma-ray spectrum data acquired by an unmanned aerial vehicle was used in the experiment. The results showed that 2D-AsLS can completely distinguish regional trend and residual values. Moreover, the trend surface fitted by 2D-AsLS can describe the regional radioactive background in detail.

Key words: airborne gamma-ray spectrometry, AsLS, regional radioactive background, trend surface fitting.

1. Introduction

Trend Surface Analysis (TSA) is widely used in the field of geochemical exploration, as it can decompose original data $\boldsymbol{Y}$ as $\mathbf{Y} = \boldsymbol{M} + \boldsymbol{V}$, where components $\boldsymbol{M}$ and $\boldsymbol{V}$ are regional trend and residual values, respectively (Wang and Zuo, 2015). Regional trend is regarded as radioactive background (that is, trend surface); while the residual values indicate local fluctuations. Maps of residual values are associated with local features of interest, e.g. mineralised anomaly. In radiological exploration work, the use of TSA for processing airborne gamma-ray spectrometry (AGS) data can eliminate the regional radioactive background in the original data and highlight the mineralisation information of the study area. At present, the polynomial least-squares method has been mostly used to fit the trend surface (Guan, 2012; Cheng *et al*., 2015; Wang and Zuo, 2015). However, a large number of application results show that when the degree of polynomial is low, fitting result cannot describe regional characteristics accurately enough. When the degree is relatively high, the method may result in overfitting.

AGS consists in mounting a detector on an aircraft (such as a fixed-wing aircraft, helicopter, etc.) to measure the radioactive element concentration in the ground from the air. Every measured value represents the average concentration of radioactive elements within a certain range of the

surface. This range is related to the flight altitude. The flight altitude of traditional AGS is usually about 120 m (IAEA TECDOC 1363, 2003). With the development of unmanned aerial vehicle (UAV), AGS based on UAV can achieve detection at low altitude. Therefore, each measurement value represents a smaller range. UAV-based AGS data are more similar to the geochemical exploration data, but the measurement method of AGS is dynamic, and the spacing between two adjacent measurement points is affected by flight speed, flight altitude, wind speed and other factors. The above factors result in an uneven distribution of the airborne gamma energy spectrum data: the distance between adjacent measurement points on the same line is approximately 10 m, while the distance between adjacent lines is approximately 100 m. This means that the spatial location of the measurement points is unevenly distributed. In order to reduce the influence of unevenly distributed data on the fitting results, the discrete data need to be gridded. Methods of gridding are various. For AGS data, IAEA TECDOC 1363 (2003) recommended method is minimum curvature. The minimum curvature method can only suppress the effect of statistical fluctuation on the data, and cannot separate the geological background information and the mineralised anomaly information.

The asymmetric least-squares method (AsLS) was first proposed by Eilers *et al.* (1996, 2006), Eilers and Marx (2003, 2010), Eilers and Boelens (2005), and Eilers (2006). AsLS is an improvement of the traditional least-squares method. Eilers *et al.* (2006) introduced the concepts of weighting coefficients and discrete roughness penalty. AsLS will determine the probability that each point belongs to the baseline, assigning different weight values to points that belong to the baseline and those that do not, i.e. fitting the signals in an asymmetric manner. AsLS has been widely adopted in the field of Raman spectral and time-resolved infrared vibrational spectral analysis to correct the baseline in spectral data (Currie *et al*., 2006; Chen *et al*., 2010; Matsubara *et al*., 2012; Mostafapour and Parastar, 2015; Lopatka *et al*., 2016). Traditionally, AsLS has been used to process 1D data; however, AGS data are 2D. In order to process data with 2D attributes by AsLS, Mostafapour and Parastar (2015) proposed a 2D AsLS algorithm. They processed the spectral data one by one, and transformed the processed data into 2D data through combination. Unfortunately, this method does not use the geodetic coordinates of data in the process of fitting the trend surface.

The overall goal of this paper is to improve AsLS and use the spatial position relationship between data points to fit a trend surface to 2D data. The key contribution of this work is that it provides a solution to build a trend surface by using 2D asymmetric least squares (2D-AsLS). This study can be applied to the field of radioactivity exploration, which can reduce the interference of geological background information on regional planning of metallogenic prospection, and has broad application prospects.

2. Material and methods

2.1. 2D-AsLS algorithm principle

AsLS is an improved method of traditional least-squares method, based on the Whittaker filter (Eilers *et al*., 1996). When fitting a trend surface of element concentration data of the airborne gamma-ray spectrum based on AsLS, let radioactive element concentration data of a certain survey line be y, and the number of measuring points on the survey line be m. Since aircrafts usually fly at a constant speed, $\boldsymbol{y}$ can be seen as the data obtained by equal interval sampling. If $\boldsymbol{\mu}$ is the trend line of $\boldsymbol{y}$, and $\boldsymbol{v}$ are the residual values in $\boldsymbol{y}$, $\boldsymbol{y}=\boldsymbol{\mu}+\boldsymbol{v}$. Let the trend line $\boldsymbol{\mu}$ be represented by tensor products of B-spline: $\boldsymbol{\mu}=\boldsymbol{B\alpha}$, where $\boldsymbol{\alpha}$ is the vector of spline coefficients, and matrix $\boldsymbol{B}$ is the spline base. The vector $\boldsymbol{\alpha}$ consisting of K columns. The matrix $\boldsymbol{B}$ consisting of m rows, and K columns.

$\boldsymbol{\alpha}$ can be estimated by linear regression, minimising S_0: $S_0 = ||\boldsymbol{y}-\boldsymbol{B\alpha}||^2$. To reduce the boundary effects and increase the fitting accuracy, Eilers *et al*. (1996) proposed P-samples. Smoothness is tuned by penalising the differences of adjacent B-spline coefficients based on the idea of a discrete roughness penalty introduced. Therefore, the optimisation objective becomes minimising *S*:

$$S = \sum_{i=1}^{m} w_i \left(y_i - \sum_{k=1}^{K} B_{ij}\alpha_k \right)^2 + \lambda \sum_{k=1}^{K} \left(\Delta^2 \alpha_k \right)^2, \tag{1}$$

where λ is the regularisation parameter, which can adjust the smoothness of the trend line; $\boldsymbol{w}$ is a scalar quantity consisting of w_i, and w_i is a weight coefficient, which indicates the probability that y_i belongs to the baseline. Given a weight coefficient p_{AsLS}, $w_i=p_{\text{AsLS}}$, if $y_i \geq \mu_i$, and w_i=1- p_{AsLS} otherwise. That is, it is possible to determine whether μ_i is part of the baseline by comparing the size of y_i and μ_i. In general, the value of p_{AsLS} is very small (0.001-0.100) (Eilers and Boelens, 2005). $\Delta^2\alpha_k$ is the differencing operator of order 2. It is assumed that $\boldsymbol{D}$ is the second derivative matrix of α_k, that is, $\boldsymbol{D}\alpha_k = \Delta^2\alpha_k$. Eq. 1 is transformed into:

$$S = \left(\boldsymbol{y} - \boldsymbol{B\alpha}\right)'\boldsymbol{W}\left(\boldsymbol{y} - \boldsymbol{B\alpha}\right) + \lambda \left\| \boldsymbol{D\alpha} \right\|^2, \tag{2}$$

where $\boldsymbol{W}$ = diag($\boldsymbol{w}$); || || is the Euclidean norm. The solution is:

$$\boldsymbol{\alpha} = \left(A_w + A_\lambda \right)^{-1} \boldsymbol{B}'\boldsymbol{W}\boldsymbol{y}, \tag{3}$$

where $A_w = \boldsymbol{B}'\boldsymbol{W}\boldsymbol{B}$, $A_\lambda = \lambda \boldsymbol{D}'\boldsymbol{D}$.

In the radioactive element concentration data of AGS, let the gridded radioactive element concentration data be matrix $\boldsymbol{Y}_{i,j}$(*n*×*m*), where *i* is the line number after gridding (*i* = 1*, …, n*), and *j* is the point number in a line after gridding (*j* = 1, …, *m*). The trend surface is the smooth surface matrix $\boldsymbol{M}$, which can be constructed by a tensor product of a P-splines (Eilers *et al.*, 2006). In matrix notation, the trend surface $\boldsymbol{M}$ can be written as: $\boldsymbol{M}=\boldsymbol{B}_l\boldsymbol{A}\,\boldsymbol{B}_p'$, where $\boldsymbol{B}_l$ (*n*×*K* matrix) is the line number direction (i.e. row direction) spline base, $\boldsymbol{B}_p$ (*m*×*L* matrix) is the point number direction (i.e. column direction) spline base, $\boldsymbol{A}$(*K*×*L*) is the coefficient matrix. *K* and *L* are the number of knots in the row and column directions of the P spline, respectively. λ becomes the regularisation parameter λ_l in the row direction and the regularisation parameter λ_p in the column direction. $\boldsymbol{D}$ becomes $\boldsymbol{D}_l$ in the row direction and $\boldsymbol{D}_p$ in the column direction. $\lambda \left\| \boldsymbol{D\alpha} \right\|^2$ becomes $\lambda_l \left\| \boldsymbol{D}_l A \right\| + \lambda_p \left\| \boldsymbol{D}_p' A \right\|_F$ in Eq. 2, with $||\cdot||_F$ is the Frobenius norm. In terms of the vectorised form of the above matrices,

$$\begin{aligned} \boldsymbol{y} &= vec\left(\boldsymbol{Y}\right), \\ \boldsymbol{\alpha} &= vec\left(\boldsymbol{A}\right), \\ \boldsymbol{\mu} &= vec\left(\boldsymbol{M}\right), \\ \boldsymbol{w} &= vec\left(\boldsymbol{W}\right), \end{aligned} \tag{4}$$

thus $\boldsymbol{A}_w$ and $\boldsymbol{A}_\lambda$ in Eq. 3 become:

$$\begin{aligned} \boldsymbol{A}_w &= \left(\boldsymbol{B}_l \otimes \boldsymbol{B}_l\right)' \boldsymbol{W}^* \left(\boldsymbol{B}_p \otimes \boldsymbol{B}_p\right), \\ \boldsymbol{A}_\lambda &= \lambda_l \left(\boldsymbol{I}_L \otimes \boldsymbol{D}_l' \boldsymbol{D}_l\right) + \lambda_p \left(\boldsymbol{D}_p' \boldsymbol{D}_p \otimes \boldsymbol{I}_K\right), \end{aligned} \tag{5}$$

where $\otimes$ is Kronecker product. $\boldsymbol{I}_L$ and $\boldsymbol{I}_K$ are unit matrix (size: $L \times L$ and $K \times K$), $\boldsymbol{W}^*$=diag($\boldsymbol{w}$). Therefore, Eq. 3 can be expanded as:

$$\boldsymbol{\alpha} = \left(\boldsymbol{A}_w + \boldsymbol{A}_\lambda\right)^{-1} \left(\boldsymbol{B}_p \otimes \boldsymbol{B}_l\right)' \boldsymbol{W}^* \boldsymbol{y}. \tag{6}$$

When the size of $\boldsymbol{Y}$ is large, the calculation speed in vectorising the matrix and in computing the Kronecker product is particularly slow. The generalised linear array models proposed by Currie *et al*. (2006) can improve computational efficiency and reduce memory usage. In Eq. 6, $\boldsymbol{A}_w$ is calculated by using the generalised linear array models. Let $\boldsymbol{A}_w = \boldsymbol{GL}$:

$$\boldsymbol{A}_w = \boldsymbol{GL} = \left[\left(\boldsymbol{e}_K \otimes \boldsymbol{B}_l\right) \circ \left(\boldsymbol{B}_l \otimes \boldsymbol{e}_K\right)\right]' \boldsymbol{W}^* \left[\left(\boldsymbol{e}_L \otimes \boldsymbol{B}_p\right) \mathrm{e} \circ \left(\boldsymbol{B}_p \otimes \boldsymbol{e}_L\right)\right]. \tag{7}$$

The size of $\boldsymbol{GL}$ is $K^2 \times L^2$, $\circ$ refers to element-by-element multiplication, $\boldsymbol{e}_K$ is a unit vector with length K, and $\boldsymbol{e}_L$ is a vector with length L. The following steps are required to obtain $\boldsymbol{A}_w$ from $\boldsymbol{GL}$: 1) transform the 2D matrix $\boldsymbol{GL}(K^2 \times L^2)$ into a 4D array $\boldsymbol{GL}_1(K \times K \times L \times L)$; 2) deformation of $\boldsymbol{GL}_1(K \times K \times \mathrm{L} \times L)$ into $\boldsymbol{GL}_2(K \times L \times K \times L)$, i.e. the second dimension elements of $\boldsymbol{GL}_1$ are interchanged with the third dimension elements; 3) transform the 4D array $\boldsymbol{GL}_2$ ($K \times L \times K \times L$) into a 2D matrix $\boldsymbol{A}_w$ ($KL \times KL$). To get vector $\left(\boldsymbol{B}_p \otimes \boldsymbol{B}_l\right)' \boldsymbol{W}^* \boldsymbol{y}$, we can create matrix $\boldsymbol{R}$, $\boldsymbol{R} = \boldsymbol{B}_p' \left(\boldsymbol{W}^* \circ \boldsymbol{Y}\right) \boldsymbol{B}_l$, and vectorise $\boldsymbol{R}$ column-wise, $\boldsymbol{r}$ = vec($\boldsymbol{R}$), and we can get $\left(\boldsymbol{B}_p \otimes \boldsymbol{B}_l\right)' \boldsymbol{W}^* \boldsymbol{y} = \boldsymbol{r}$.

Algorithm implementation and data computation are based on MATLAB 2019a (9.6.0). The discrete data gridding is based on SURFER v15. Figs. 1 and 3 are drawn by SURFER v15. Fig. 2 is drawn by OriginPro 2017C (9.4.2).

2.2. Field data

The experimental instrument adopts a UAV gamma-ray spectrum measurement system. It was jointly developed by Chengdu University of Technology and Chengdu New Ray Technology Co., Ltd. The system was installed at the bottom of the UAV, including a one-litre sodium iodide (NaI) crystal, a two-litre sodium iodide (NaI) crystal, a photomultiplier tube and related circuits. The UAV has a flight altitude of 80 m, flight speed of 10 m/s, and sampling time of 1 s. The radioactive element concentration data was obtained from the accumulative spectrum of the two crystals.

The study area is located in a prospective metallogenic area in Jiangxi province, China, covering an area of about 2.2 km^2. There are 2622 sets of survey data, including GPS coordinates, GPS height, radar height, concentration of U, Th and K, etc. The detector was calibrated by a standard device for radioactive measurement models (the device is a Chinese secondary standard device, located in Sichuan, China). The raw measurement data was pre-processed according to the method recommended by IAEA TECDOC 1363 (2003). This paper takes U element data as experimental data to study the effect of 2D-AsLS on the fitting of trend surface. The U element data was gridded to form a data matrix $\boldsymbol{Y}$ with n = 50 in the measurement line direction and m = 100 in the measurement point direction. The gridding method uses the minimum curvature that is recommended by IAEA TECDOC 1363 (2003). About the parameter of minimum curvature,

maximum residual is 0.22, maximum iteration is 100,000. In the processed data, the average value of U concentration is 10.34 μg/g. The lowest value is 0 μg/g (replace with 0 if lower than 0, the negative values occur because the measured values are lower than the background values). After gridding, the highest value in the original data changed from 179.1 to 164.6 μg/g. The sketch of the flight track in the survey area is shown in Fig. 1a. The contour map after gridding is shown in Fig. 1b.

In Fig. 1b, anomaly area of U concentration is present in the study area. The anomaly has a halo-like distribution and a trend towards high enrichment. These characteristics are similar to those of mineralised anomaly. This anomaly area is superimposed on the median area of 40-60 μg/g. This median area spans the entire study area and is distributed roughly along a N-S direction. At the same time, the median area is mainly located in the eastern part of the study area, with sporadically distributed point-like high value anomalies within the median area. To determine the cause of these anomalies, it is necessary to do further analysis of the study area data.

2.3. Selection of optimal parameters

When using 2D-AsLS to fit trend surface of the radioactive element concentration data, the parameters in 2D-AsLS will determine the effect of trend surface fitting. These parameters include weight p_{AsLS}, knots number $nseg_l$ in line direction and knots number $nseg_p$ in point direction of P-spline, smoothness λ_l in line direction and smoothness λ_p in point direction.

In the data matrix $\boldsymbol{Y}$, the spacings between a point and its neighboring points in row direction or column direction are equal, i.e. the spatial scale of $\boldsymbol{Y}$ in row direction and column direction are the same. Thus, the smoothness in row direction and column direction is the same, i.e. $\lambda = \lambda_l = \lambda_p$. The number of knots in P-spline determines the accuracy and computation time in the trend surface (Eilers, 2006). High accuracy means more calculation time. To balance the accuracy and

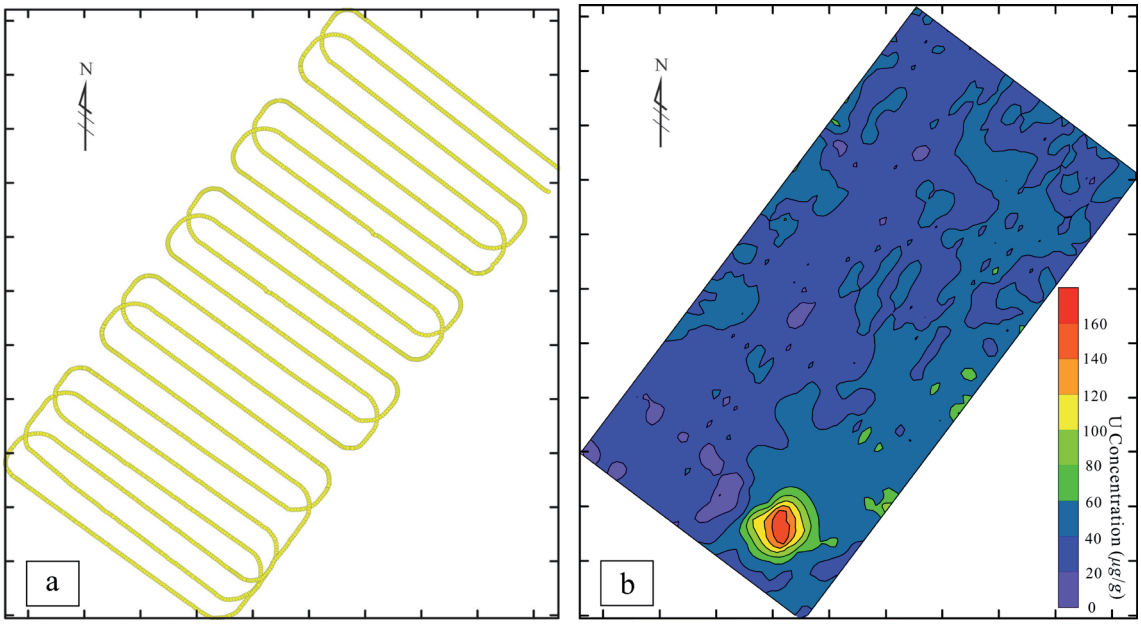

Fig. 1 - The flight track sketch of UAV in the gamma-ray spectrum survey area (a) and contour map of the original U concentration after gridding (b).

computation time, $nseg_l$ and $nseg_p$ are taken as n and m, respectively. Therefore, the parameters that need to be adjusted are only weight p_{AsLS} and smoothness λ.

Due to the complexity of the metallogenic process and the ever-changing geological structure of the mining area, there is still no unified geological model to describe the geological structure of a mining area. Therefore, it is difficult to select the optimal parameters by establishing a unified geological model of mining area. To solve the above problems, the authors selected the optimal parameters based on the characteristics of the data and a variety of evaluation methods. In this paper, fitting coefficient (R^2), error variance (σ^2), coefficient of variation (CV) and degree of deviation (N) were used to evaluate the fitting effect of trend surface to select optimal parameters. Let the trend surface matrix be $\boldsymbol{M}_{i,j}$, the gridded data matrix be $\boldsymbol{Y}_{i,j}$, the mean value of $\boldsymbol{Y}$ be $\bar{y}$.

1) Fitting coefficient: R^2

$$R^2 = 1 - \frac{\sum_{i=1}^{n}\sum_{j=1}^{m}\left(\boldsymbol{Y}_{i,j} - \boldsymbol{M}_{i,j}\right)^2}{\sum_{i=1}^{n}\sum_{j=1}^{m}\left(\boldsymbol{Y}_{i,j} - \bar{y}\right)^2} \quad . \tag{8}$$

The fitting coefficient is an important indicator to evaluate the fitting effect of the regression model, and it expresses the overall relationship between trend surface and data matrix. The closer the R^2 is to 1, the more similar the trend surface and data matrix are.

2) Error variance: σ^2

$$\sigma^2 = \frac{1}{m \times n}\sum_{i=1}^{n}\sum_{j=1}^{m}\left(\boldsymbol{Y}_{i,j} - \boldsymbol{M}_{i,j}\right)^2 . \tag{9}$$

The variance σ^2 can evaluate the similarity between trend surface and data matrix. σ^2 is negatively correlated with fitting degree.

3) Coefficient of variation for M: CV

$$CV = \frac{\sigma}{\overline{M}} . \tag{10}$$

CV can evaluate the distribution of data and it is a dimensionless quantity. CV is negatively correlated with the concentration degree of element distribution on the trend surface.

4) Degree of deviation: N

$$N = \frac{N_{neg}}{n \times m} \times 100\% . \tag{11}$$

N_{neg} is the number of negative points in the matrix $\boldsymbol{M}$. The value of radioactive element concentration is non-negative, but when fitting the trend surface, at some grid nodes negative values of the fitted surface may occur in the trend surface $\boldsymbol{M}$. These negative values are clearly contrary to the reality. N is a quantity that measures the proportion of negative points in the matrix, which can be used to evaluate the reliability of the fitting results.

According to the range of p_{AsLS} values recommended by Eilers and Boelens (2005), this analysis calculated different evaluation parameters when p_{AsLS} is 0.1, 0.01, and 0.001 (the results are shown in Table 1). The results show that the weight parameter p_{AsLS} has little effect on fitting trend surface. Therefore, let p_{AsLS} = 0.001 (because *N* is minimal).

Table 1 - Relevant parameters of trend surface fitted by 2D-AsLS for different p_{AsLS} values (λ = 40).

Parameters	p_{AsLS} value		
	0.1	0.01	0.001
R^2	0.6590	0.6602	0.6659
σ^2	92.79	92.54	92.26
CV	1.30	1.29	1.27
N	0.095	0.092	0.089

Therefore, only smoothness *λ* has an effect on the fitting. We calculated the four evaluation parameters of the trend surface obtained by fitting different *λ*, and calculated the slope of the line segment formed by two adjacent points. The results are shown in Fig. 2.

In Fig. 2, the black squares are the calculated values of the evaluation parameters and the red dashed lines are the fitted lines of the trend of the calculated values. In Fig. 2a, the rate of

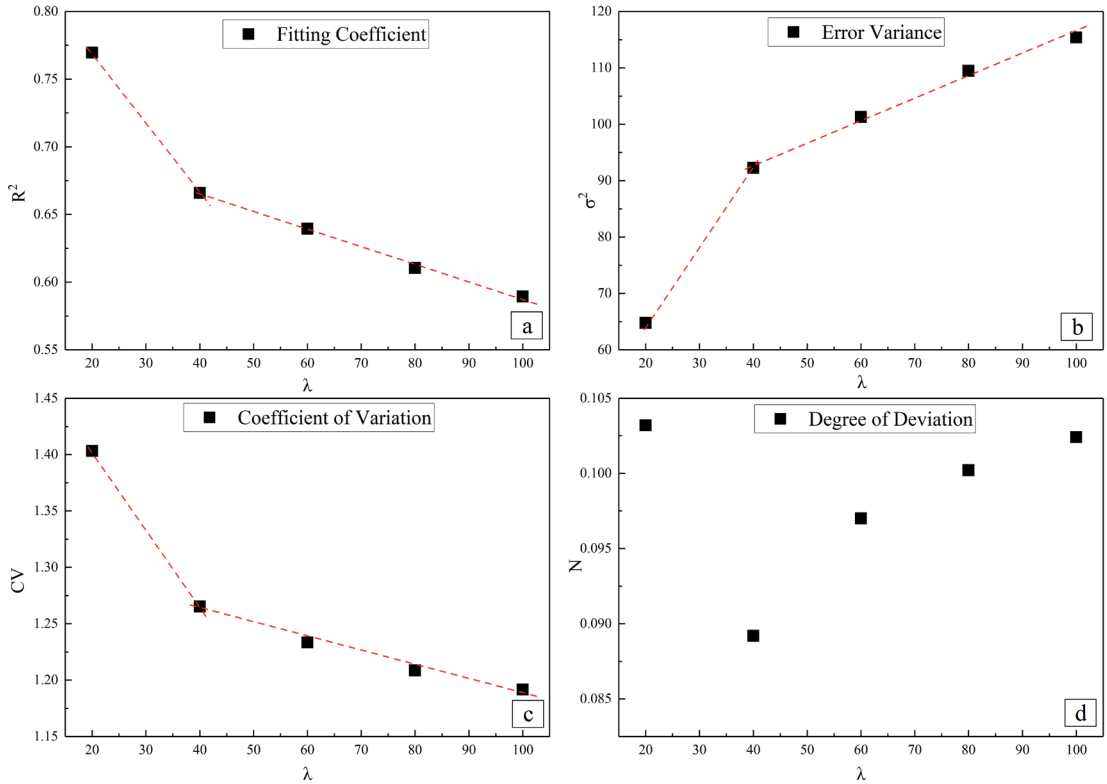

Fig. 2 - The values of the evaluation parameter of the trend surface at different *λ* values: a) Fitting coefficient; b) Error variance; c) Coefficient of variation; d) Degree of deviation.

change of R^2 as λ changes from 20 to 40 is significantly different from the rate of change of R^2 as λ changes from 40 to 100. When $\lambda < 40$, R^2 changes rapidly with λ. This is due to the fitted trend surface that still contains mineralised anomaly, and changes in λ affect the proportion of mineralised anomaly in the trend surface. When $\lambda > 40$, R^2 changes slowly with λ. This is due to the fitted trend surface that does not contain mineralised anomaly, and changes in λ only affect the fineness of the trend surface. Similarly, the same trend is seen in Figs. 2b and 2c. In Fig. 2d, when $\lambda = 40$, N is minimum. $\lambda = 40$ is the optimal parameter.

3. Result and discussion

3.1. Conventional method for fitting trend surfaces

At present, the traditional method for fitting trend surface is polynomial least squares (Guan, 2012; Cheng *et al*., 2015; Wang and Zuo, 2015). The formula for fitting the trend surface matrix $\boldsymbol{M}$ by polynomial least squares is:

$$\boldsymbol{M}=k_{00}+k_{10}x_i+k_{01}y_i+k_{20}x_i^2+k_{11}x_iy_i+\ldots+k_{pq}x_i^py_i^q \quad (12)$$

where, k_{00} to k_{pq} are coefficients of the polynomial, p is the degree of the polynomial in X direction, and q is the degree of the polynomial in Y direction. The goodness-of-fit is evaluated by R^2 (Wang and Zuo, 2015).

Using third-degree polynomials to fit the trend surface $\boldsymbol{M}$, the fitted $R^2 = 0.3251$.

3.2. Comparison of fitting results

In order to compare the fitting results of the trend surfaces by the two methods, we fitted the trend surfaces by 2D-AsLS and third-degree polynomials, respectively, and the gridded data was separated into two parts: the regional trend part and the residual part. The fitting results by 2D-AsLS are shown in Fig. 3 and the fitting results by third-degree polynomials are shown in Fig. 4.

Figs. 3a and 4a are the same as in Fig. 1b. As shown in Fig. 3, after 2D-AsLS fitted, the shape of the trend surface resulted similar to the shape of the gridded data. In Fig. 3b, the several scattered anomalies (60-100 μg/g) in the central area have connected the low value halo in the SE corner of the study area, and the range of the anomaly has increased and their intensity has decreased. This suggests that during the process of fitting the trend surface by 2D-AsLS, sporadic point anomalies are gradually weakened by the trend surface and are eventually identified as geological background information. For the anomaly area in the south-eastern part of the study area, although the intensity of the anomaly decreases after fitting by 2D-AsLS, the shape and range of the anomaly remained unchanged, which indicates that the 2D-AsLS could identify anomalies with different intensities. At the same time, the centre of the concentration anomaly is not obviously connected to or offset from the boundary of the study area, which indicates that this method is less affected by boundary effects. In Fig. 3c, the shape and position of the anomaly with halo-like distribution has not changed, and the sporadically distributed point-like high value anomalies have completely disappeared.

As shown in Fig. 4, after third-degree polynomials fitted, the shape of the trend surface was significantly different from the shape of the gridded data. In Fig. 3b, the distribution of the

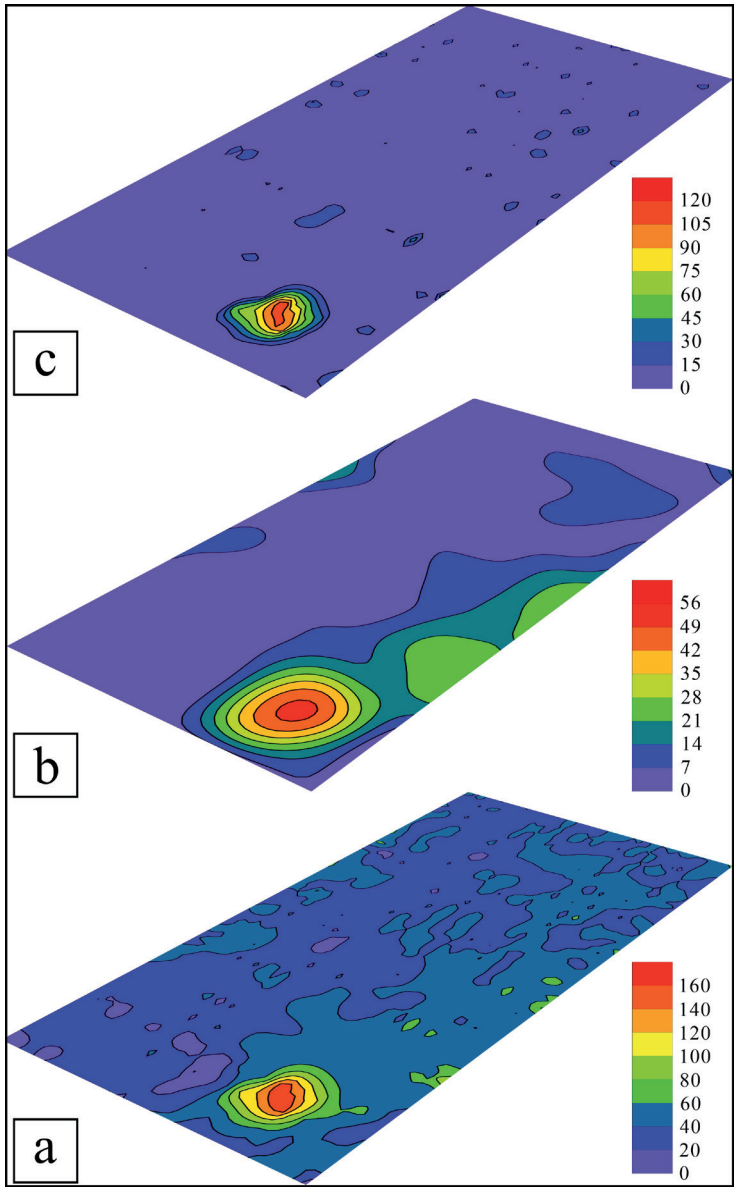

Fig. 3 - The fitting results by 2D-AsLS (Unit: μg/g): original U concentration data after gridding (a), trend surface fitted by 2D-AsLS (λ = 40) (b) and residual values (c).

anomalous area is elliptical with a N-S direction, and the description of the geological background information on the trend surface is simple and inaccurate. Because of boundary effects, the centre of the high-value anomalous halo in the southern part of the study area is shifted towards the boundary and the area of the anomalous halo is increased. The several scattered anomalies (60-100 μg/g) in the central area have connected the high value halo in the SE corner of the study area. The area of the anomaly halo has increased and its intensity has decreased. In Fig. 3c, the position of the anomaly with halo-like distribution has shifted towards the eastern part of the study area, but the shape of the anomaly has not changed. This is due to the centre of the high-value anomaly halo on the trend surface shifting towards the boundary.

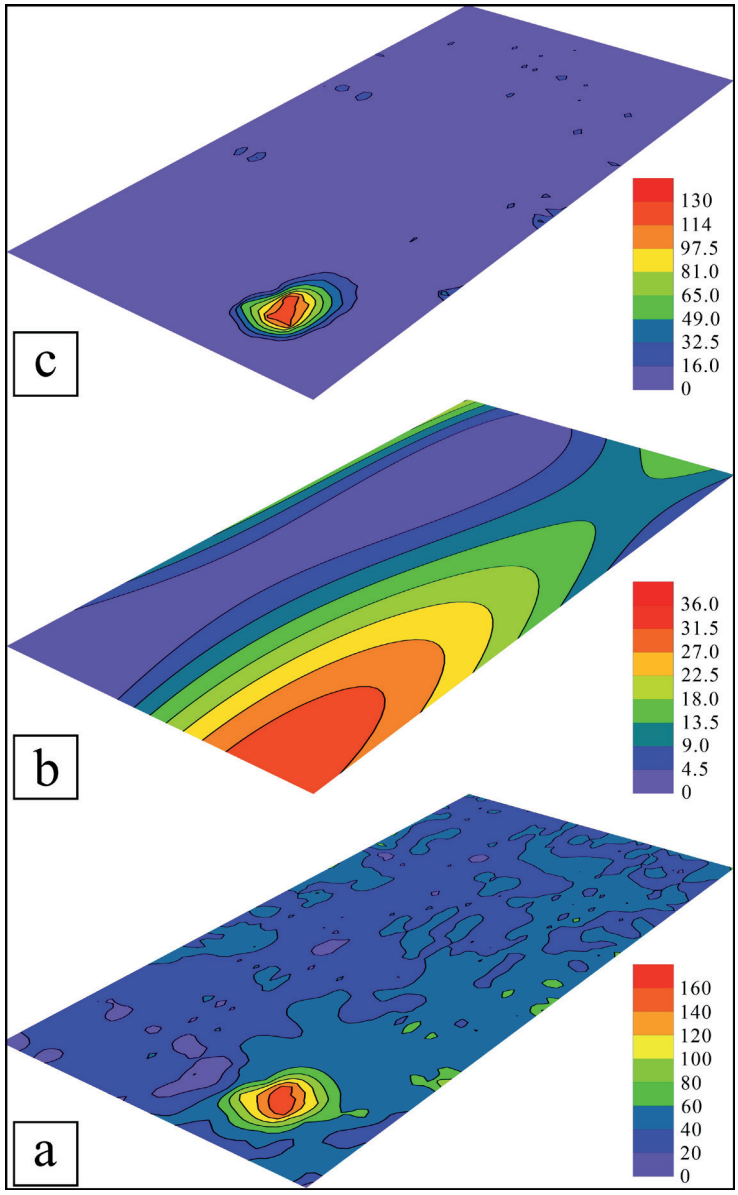

Fig. 4 - The fitting results by third-degree polynomials (Unit: μg/g): original U concentration data after gridding (a), trend surface fitted by third-degree polynomials (b) and residual values (c).

The R^2 of 2D-AsLS is 0.69, which is much better than the R^2 of polynomial (0.33). Therefore, in terms of separate the regional trend and the residual value in the original data, 2D-AsLS is better. The above analysis shows that the third-degree polynomials cannot accurately describe the geological background information, and that the method is strongly affected by boundary effects. On the other hand, the 2D-AsLS can describe the geological background information at a fine scale, and that the method is less affected by boundary effects. After filtering the geological background information from the gridded data, the mineralogical anomaly information can be retained in a more complete way in the residual values.

4. Conclusions

AsLS has been successfully applied in the field of spectral analysis. The radioactive element concentration data obtained by airborne gamma-ray spectrum contains the spatial position information (x and y), which indicates the spatial position relationship between data points. However, the traditional AsLS algorithm does not make full use of this information. Therefore, using AsLS to fit the trend surface of radioactive element concentration cannot accurately describe the regional radioactive background. To this end, we improve AsLS by using the 2D tensor product of P-splines, and propose a trend surface analysis model based on 2D-AsLS.

The 2D-AsLS parameter λ can influence the fitting results of the trend surface, for which we used four parameters to evaluate the fitting results in order to find the optimal parameter values. The effect of the trend surface fitted by AsLS is demonstrated by using the measured U concentration data from the AGS. The results show that trend surfaces fitted by 2D-AsLS can describe the geological background information at a finer scale and less affected by boundary effects. After filtering the geological background information from the gridded data, the mineralogical anomaly information can be retained in a more complete way in the residual values. This method can be used as an alternative to traditional methods in TSA, enriching the technical means of AGS data analysis, and reducing the interference of geological background information on regional planning of metallogenic prospection.

Acknowledgement. The authors acknowledge the financial support by the Sichuan Science and Technology Program (Project No. 2020JDRC0108), the National Science Foundation of China (Project No. 41774147 and Project No. 41774190).

REFERENCES

Chen S., Li X.N., Liang Y.Z., Zheng Z.M., Liu Z.X., Zhang Q.M., Ding L.X. and Ye F.; 2010: *Raman spectroscopy fluorescence background correction and its application in clustering analysis of medicines*. Spectrosc. Spectral Anal., 30, 2157-2160, doi: 10.3964/j.issn.1000-0593(2010)08-2157-04, 9 (in Chinese).

Cheng J.Y., Li B.F., Fan T. and Liu L.; 2015: *TEM weak anomalies extracting method based on trend surface analysis*. J. China Coal Soc., 40, 2856-2864, doi: 10.13225/j.cnki.jccs.2015.0232.

Currie I.D., Durbán M. and Eilers P.H.C.; 2006: *Generalized linear array models with applications to multidimensional smoothing*. J. R. Stat. Soc.: Ser. B, 68, 259-280, doi: 10.1111/j.1467-9868.2006.00543.x.

Eilers P.H.C.; 2006: *Unimodal smoothing*. J. Chemom., 19, 317-328, doi: 10.1002/cem.935.

Eilers P.H.C. and Boelens H.F.M.; 2005: *Baseline correction with asymmetric least squares smoothing*. Leiden University Medical Centre, Leiden, The Netherlands, Technical Report, 24 pp.

Eilers P.H.C. and Marx B.D.; 2003: *Multivariate calibration with temperature interaction using two-dimensional penalized signal regression*. Chemom. Intell. Lab. Syst., 66, 159-174, doi: 10.1016/s0169-7439(03)00029-7.

Eilers P.H.C. and Marx B.D.; 2010: *Splines, knots, and penalties.* WIREs Comput. Stat., 2, 637-653, doi: 10.1002/wics.125.

Eilers P.H.C., Rijnmond D.M. and Marx B.D.; 1996: *Flexible smoothing with B-splines and penalties*. Stat. Sci., 11, 89-121, doi: 10.1214/ss/1038425655.

Eilers P.H.C., Currie I.D. and Durbán M.; 2006: *Fast and compact smoothing on large multidimensional grids*. Comput. Stat. Data Anal., 50, 61-76, doi: 10.1016/j.csda.2004.07.008.

Guan R.R.; 2012: *The study of trend surface analysis*. China Min. Mag., 21, 474-478.

IAEA TECDOC 1363; 2003: *Guidelines for radioelement mapping using gamma ray spectrometry data*. International Atomic Energy Agency, Vienna, Austria, 171 pp., <www.iaea.org/publications/6746/guidelines-for-radioelement-mapping-using-gamma-ray-spectrometry-data>.

Lopatka M., Barcaru A., Sjerps M.J. and Vivó-Truyols G.; 2016: *Leveraging probabilistic peak detection to*

estimate baseline drift in complex chromatographic samples. J. Chromatogr. A, 1431, 122-130, doi: 10.1016/j.chroma.2015.12.063.

Matsubara Y., Yoshida T., Ishikawa T., Okimoto Y., Koshihara S.Y. and Onda K.; 2012: *Photoinduced ionic to neutral phase transition in TTF-CA studied by time-resolved infrared vibrational spectroscopy*. Acta Phys. Pol. A, 121, 340-342, doi: 10.12693/APhysPolA.121.340.

Mostafapour S. and Parastar H.; 2015: *N-way partial least squares with variable importance in projection combined to GC×GC-TOFMS as a reliable tool for toxicity identification of fresh and weathered crude oils*. Anal. Bioanal. Chem., 407, 285-295, doi: 10.1007/s00216-014-8076-1.

Wang H.C. and Zuo R.G.; 2015: *A comparative study of trend surface analysis and spectrum-area multifractal model to identify geochemical anomalies*. J. Geochem. Explor., 115, 84-90, doi: 10.1016/j.gexplo.2015.04.013.

Corresponding author: Liang Quan Ge
The College of Nuclear Technology and Automation Engineering, University of Technology
No.1, Erxianqiao East Third Road, Chengdu 610059, China
Phone: +86 136 7815 7263; email: glq@cdut.edu.cn